DOI: 10.1002/chem.200501235

Single and Double pH-Driven Cu^{2+} Translocation with Molecular Rearrangement in Alkyne-Functionalized Polyamino Polyamido Ligands

Annalisa Aurora,[a] Massimo Boiocchi,[b] Giacomo Dacarro,[c] Francesco Foti,[c] Carlo Mangano,[c] Piersandro Pallavicini,*[c] Stefano Patroni,[c] Angelo Taglietti,[c] and Robertino Zanoni[a]

Abstract: A new series of ligands, containing one (**L1**H_2–**L4**H_2) or two (**L5**H_4–**L6**H_4) 1,4,8,11-tetraaza-5,7-dione units and functionalized with a propargyl group on the C atom between the C=O moieties, has been synthesized. Protonation constants for the ligands and formation constants of their Cu^{2+} complexes have been determined in water, and the coordination geometry of the complexes existing at various pH values has been investigated by coupled pH-metric and spectrophotometric titrations. Ligands capable of simple uptake of Cu^{2+} with the formation of neutral, square-planar complexes containing the −2-charged diamino-diimido donor sets and ligands containing further coordinating groups (quinoline or pyridine) capable of single and double cation translocation have been investigated. The role of the substituents on the amino groups and the structural role played by the propargyl group have been examined as regards Cu^{2+} complexation and translocation. In the double-translocating ligand **L6**H_4, when the two Cu^{2+} ions move inside the diamino-diamido donor set, the slim propargyl group allows an unprecedented folding of the whole ligand with apical coordination of one pyridine to form a five-coordinate, square-pyramidal Cu^{2+} ion. The crystal and molecular structures of this unusual [**L6**Cu_2] complex have been determined by X-ray diffraction. Finally, oxidation of Cu^{2+} to Cu^{3+} has been studied by cyclic voltammetry in water, which revealed that the redox reaction occurs only when the copper cation is within the diamino-diimido compartment. Moreover, both functionalization of the primary amines with bulky substituents and apical coordination of Cu^{2+} make access to the 3+ oxidation state more difficult and disrupt the reversibility of the electrochemical process.

Keywords: copper · ion translocation · macrocyclic ligands · molecular devices · molecular machines

Introduction

Open and cyclic diamino-diamido ligands have been known for almost 30 years.[1] They have been studied in detail because of their unique features: 1) they are poor ligands in slightly acidic or neutral aqueous solution (in their **L**H_2 form) but at sufficiently high pH interaction with an appropriate M^{2+} metal ion switches them to a powerful binding system: the two amido protons are released giving the ligands a diamino-diimido dinegative four-donor set capable of forming very stable, neutral, [M**L**] square-planar complexes (see Scheme 1 A);[2] 2) they are selective: among first-row transition-metal cations only Ni^{2+} and Cu^{2+} (thanks to their particularly high charge/dimension ratio and crystal field stabilization energy (CFSE)) are capable of promoting the endoergonic deprotonation of the amido groups to form [M**L**] complexes; 3) when coordinated by the dinegative donor set in these ligands, Ni^{2+} and Cu^{2+} can be oxidized to the unusual +3 oxidation state: the strong in-plane donor–metal interactions and the dinegative charge of the ligand promote the process, which is electrochemically reversible in a number of solvents, including water;[3] 4) they allow facile synthetic modifications: the most commonly em-

[a] Dr. A. Aurora, Prof. R. Zanoni
Dipartimento di Chimica 4
Università degli Studi di Roma "La Sapienza"
P.le Aldo Moro, 5–00185 Roma (Italy)

[b] Dr. M. Boiocchi
Centro Grandi Strumenti
via Bassi 21–27100 Pavia (Italy)

[c] Dr. G. Dacarro, Dr. F. Foti, Dr. C. Mangano, Dr. P. Pallavicini, Dr. S. Patroni, Dr. A. Taglietti
Dipartimento di Chimica Generale
Università di Pavia
via Taramelli, 12–27100 Pavia (Italy)
Fax: (+39) 0382-528-544
E-mail: psp@unipv.it

Supporting information for this article is available on the WWW under http://www.chemeurj.org/ or from the author.

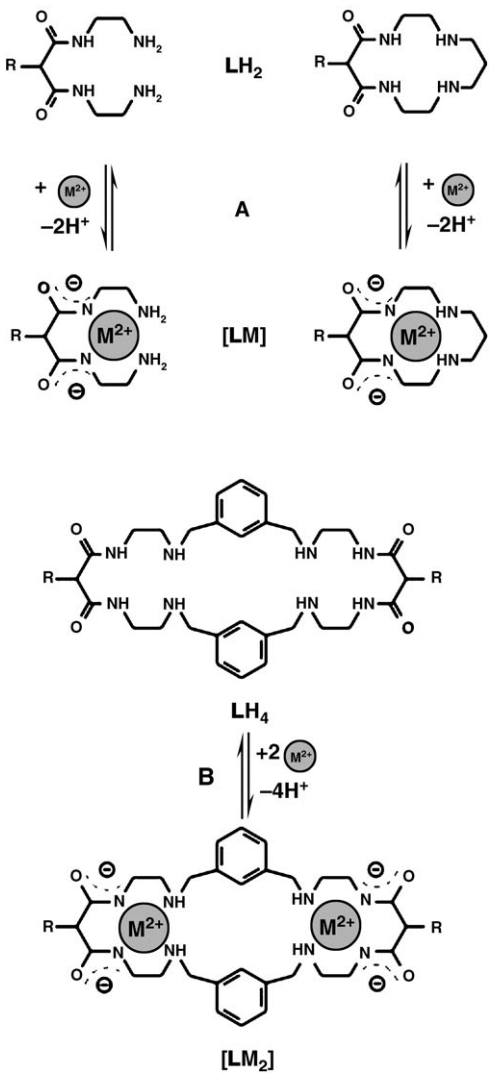

Scheme 1. Formation equilibria for the neutral complexes with one or two metal cations in ligands containing one or two 1,4,8,11-tetraaza-5,7-dione units; M^{2+} = Ni^{2+} or Cu^{2+}.

ployed diamino-diamido ligands contain the 1,4,8,11-tetraaza-5,7-dione framework (as in the examples shown in Scheme 1), which can be easily monofunctionalized in the 6-position with a huge variety of molecular groups (R in Scheme 1).

In addition the primary or secondary amines can be derivatized, and the ligands obtained maintain their unique coordinative features. Photochemical[4] and electrochemical sensors[5] for Ni^{2+} and Cu^{2+} have been built using this framework. Moreover, recently some of the authors of this article in collaboration with Fabbrizzi et al. have demonstrated that owing to the intrinsically pH-switchable nature of these ligands, appending two further coordinating groups to the primary amines (e.g. pyridines, quinolines, bipyridines) results in either open[6] or cyclic[7] molecules in which intramolecular Ni^{2+}[6a–b] or Cu^{2+}[6c–d,7] translocation is driven by pH.

Notably, we and Fabbrizzi[7] have shown that in a system in which double Cu^{2+} translocation is observed, the imidazolate anion can be taken up and released as a result of the cation's movement, opening the path to pH-driven molecular machines capable of acting as receptors that can be open and closed on command. Focusing on Cu^{2+} translocation, we and Fabbrizzi have demonstrated[6c] that appending a pyridine group to the 1,4,8,11-tetraaza-5,7-dione framework gives a system in which cation translocation is accompanied by molecular folding, with Cu^{2+} being unusually five-coordinate even inside the diamino-diimido compartment (Scheme 2, form **A2**), thanks to the chelating effect exerted by the pyridine group. In contrast, when two ligands of this kind are merged within a single macrocyclic structure, folding of the pyridine groups is not observed and double translocation inside the diamino-diimido compartments gives two truly square planar Cu^{2+} ions[7] (Scheme 2, form **B2**).

Our goals include the ability to control the shape of a molecule when one or more cations change position inside it on command and to tune the coordination number and geometry of the moving cations in their different positions. In the long term, our aim is to prepare self-assembled monolayers (SAMs) of these molecular systems on conducting or semiconducting surfaces. The overall shape and charge of the molecular systems, the coordination number and geometry of the metal center(s), and the metal–metal distance inside a single molecule can strongly influence interesting properties of the functionalized surface, including conductivity, electrical capacity, and color.[8] Along these lines, we have now synthesized the **L1**H_2–**L6**H_4 series of new ligands based on the 1,4,8,11-tetraaza-5,7-dione framework and featuring the propargyl group between the carboxy moieties. Propargyl is a very useful functional group for the prospective further step of preparing SAMs of these molecules on Si surfaces.[8b] In addition, $HC{\equiv}C{-}CH_2{-}$ is short relative to the groups we have previously appended in the same position: it imparts only a modest hydrophobicity to the functionalized ligands and, owing to its cylindrical nature, it exerts little steric hindrance. Accordingly, we wanted to understand how the limited bulkiness of propargyl influences the overall shape of the copper complexes and the Cu^{2+} coordination geometry in the various positions between which the cation(s) is allowed to move. We have thus undertaken a detailed characterization of the complexes, and of the spectral and electrochemical properties of all of these ligands towards Cu^{2+} in water, and examined the pH-driven translocating capabilities of **L4**H_2 and **L6**H_4. The coordination constants of the Cu^{2+} complexes formed by all of the ligands in water solution in the pH range 2–12 have been calculated and the coordination number and geometry of the complexes have been established. Moreover, the crystal and molecular structures of the diimino-diimido Cu^{2+} complexes of **L1**H_2 and **L6**H_4 have been determined by X-ray diffraction.

Results and Discussion

Complexation processes in non-translocating systems: After determining the protonation constants of all of our ligands

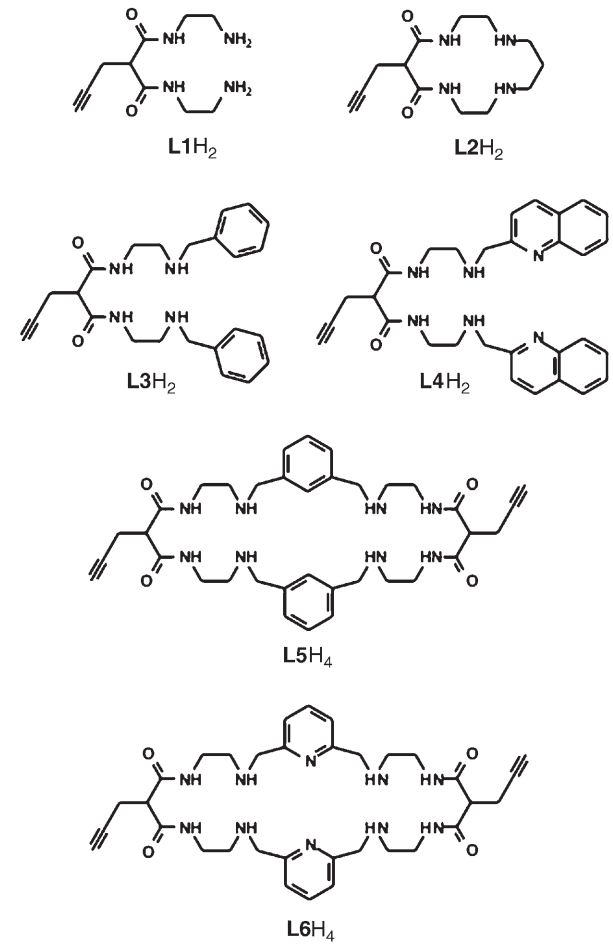

(see Supporting Information, Table S1), we examined the complexation tendencies of **L1**H_2–**L3**H_2 and **L5**H_4 towards Cu^{2+} in aqueous solutions (0.05 M $NaNO_3$) containing ligand and one (**L1**H_2–**L3**H_2) or two equivalents (**L5**H_4) of [Cu-$(CF_3SO_3)_2$]. Excess HNO_3 was also added and potentiometric titrations were carried out by addition of standard NaOH. Data refinement (Hyperquad package[9]) allowed us to determine the formation constants of the species existing in the 2–12 pH range. The logarithmic values of the constants and the formation equilibria to which they are referred are listed in Table 1.

L1H_2 is the simplest ligand of the set we examined: it is acyclic and its two amino groups are unsubstituted (primary). From the formation constants listed in Table 2 and the protonation constants in Table S1 (see Supporting Information), a distribution diagram (% of species with respect to total **L1**H_2 versus pH) may be drawn (Figure 1 A), showing that only two dominant species exist in the 2–12 pH range, the diprotonated ligand $[\mathbf{L1}H_4]^{2+}$ and the neutral, square-planar complex with deprotonated amido groups [**L1**Cu]. The protonation and formation constants of the species that we have identified in the pH 2–12 range and, as a consequence, the resulting distribution diagram are similar to those previously described for plain 1,4,8,11-tetraaza-5,7-dione and for its 6-benzyl analogue.[10]

It must be stressed that the $[\mathbf{L1}H_2Cu]^{2+}$ complex, though existing in the pH range examined, is unstable and reaches a concentration of only 20 %. This is in accord with its formation constant, which is low (7.60 log units) considering that it is a diamino ligand coordinating a single Cu^{2+} ion. This value is comparable with the logβ_2 value of 7.51 reported in the literature for methylamine[11] and indicates that the two primary amines, separated by a chain of nine atoms, are not profiting from any chelate effect. The hydroxide-coordinated compound $[\mathbf{L1}H_2Cu(OH)]^{+}$ forms in an even lower quantity (< 15 %) and can be considered to be forming from $[\mathbf{L1}H_2Cu]$ by deprotonation of one of the water molecules that complete the coordination sphere of the Cu^{2+} ion (pK_a = 6.46). In contrast, the [**L1**Cu] species is a square-planar, neutral complex with two deprotonated amido groups on the ligand framework, as described in Scheme 1 for R = $-CH_2C{\equiv}CH$. This is clearly demonstrated by the visible band of the complex, which is centered at 518 nm

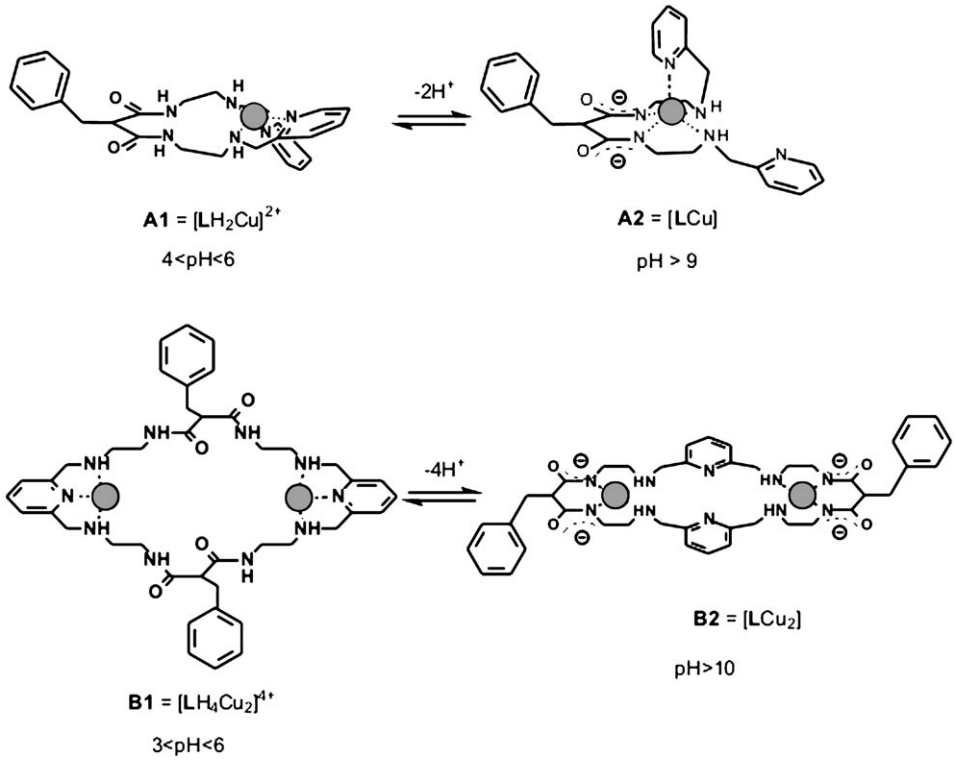

Scheme 2. Equilibria involved in the pH-driven translocation plus folding of one Cu^{2+} ion and in the translocation of two Cu^{2+} ions.

Table 1. Formation constants (and relevant equilibria) for the species present in solution for ligands $\mathbf{L1}H_2$–$\mathbf{L3}H_2+Cu^{2+}$ (1:1 molar ratio) and $\mathbf{L5}H_4+Cu^{2+}$ (1:2 molar ratio). Uncertainties are reported in parentheses.

	$\mathbf{L1}H_2$	$\mathbf{L2}H_2$	$\mathbf{L3}H_2$	$\mathbf{L5}H_4$
$\mathbf{L}H_2+Cu^{2+}\rightleftharpoons[\mathbf{L}H_2Cu]^{2+}$	7.60(0.01)	8.34(0.01)	5.97(0.01)	
$\mathbf{L}H_2+Cu^{2+}+H_2O\rightleftharpoons[\mathbf{L}H_2Cu(OH)]^{+}+H^{+}$	1.14(0.01)	4.59(0.01)	0.06(0.01)	
$\mathbf{L}H_2+Cu^{2+}\rightleftharpoons[\mathbf{L}Cu]+2H^{+}$	−4.71(0.01)	−1.21(0.01)	−4.99(0.02)	
$\mathbf{L}H_4+2Cu^{2+}\rightleftharpoons[\mathbf{L}H_4Cu_2]^{4+}$				11.39(0.01)
$\mathbf{L}H_4+2Cu^{2+}+2H_2O\rightleftharpoons[\mathbf{L}H_4Cu_2(OH)_2]^{2+}+2H^{+}$				−0.84(0.01)
$\mathbf{L}H_4+2Cu^{2+}\rightleftharpoons[\mathbf{L}Cu_2]+4H^{+}$				−14.18(0.01)

Table 2. Crystal data for investigated crystals.

	[**L1**Cu]·2(H_2O)	[**L6**Cu_2]·9(H_2O)
formula	$C_{10}H_{20}CuN_4O_4$	$C_{68}H_{102}Cu_4N_{20}O_{17}$
M_r	323.85	1725.86
color	violet	violet
dimensions [mm]	0.75×0.55×0.35	0.25×0.18×0.14
crystal system	orthorhombic	monoclinic
space group	*Pbnm* (no. 62)	*C*2/*c* (no. 15)
a [Å]	9.499 (4)	26.866 (8)
b [Å]	10.480(4)	14.464(4)
c [Å]	13.403(6)	24.638(10)
β [°]	–	125.57(5)
V [Å^3]	1334.3(10)	7787.8(72)
Z	4	4
ρ_{calcd} [g cm^{-3}]	1.612	1.472
μ $Mo_{K\alpha}$ [mm^{-1}]	1.654	1.156
scan type	ω–2θ scans	ω scans
θ range [°]	2–30	2–25
measured reflections	2018	7008
unique reflections	2018	6823
R_{int}[a]	–	0.0999
strong reflections [$I_O>2\sigma(I_O)$]	1713	2220
*R*1, *wR*2 (strong data)[b]	0.0282, 0.0726	0.0962, 0.1728
*R*1, *wR*2 (all data)[b]	0.0372, 0.0768	0.2883, 0.2350
GOF[c]	1.053	0.936
refined parameters	104	537
max/min residuals [e Å^{-3}]	0.39/−0.37	0.60/−0.48

[a] $R_{int}=\Sigma|F_o^2-F_o^2(mean)|/\Sigma F_o^2$. [b] $R1=\Sigma||F_o|-|F_c||/\Sigma|F_o|$, $wR2=[\Sigma[w(F_o^2-F_c^2)^2]/[\Sigma w(F_o^2)^2]]^{1/2}$, in which $w=1/[\sigma 2F_o^2+(aP)^2+bP]$ and $P=[(Max(F_o^2,0)+2F_c^2)^2]/3$. [c] $GOF=[\Sigma[w(F_o^2-F_c^2)^2]/(n-p)]^{1/2}$, in which *n* is the number of reflections and *p* the total number of refined parameters.

(ε = 60 M^{-1} cm^{-1}; see Figure S1 in the Supporting Information for a UV/Vis spectrum recorded at pH 8.5) and imparts a characteristic pink color to the complex. As previously described in the literature, the unusually high energy (at least for a Cu^{2+} amino complex) of this band is due to the square-planar geometry of the complex and to the particularly strong in-plane ligand–metal interactions exerted by the diamino-diimido donor set, which give rise to an unusually large separation in the d orbitals involved in the d–d transition.[1] The wavelength of the maximum absorption compares well with that reported for 1,4,8,11-tetraaza-5,7-dione (λ_{max} = 516 nm) and 6-benzyl-1,4,8,11-tetraaza-5,7-dione (λ_{max} = 520 nm).[10] Moreover, the crystal and molecular structure found by X-ray diffraction confirms what is found in solution (see Figure S2 in the Supporting Information) and shows that in [**L1**Cu] the Cu^{2+} ion is four-coordinate and almost perfectly square-planar, with only a very slight pyramidal distortion. The four nitrogen donor atoms lie in the same plane, and the Cu^{2+} ion is displaced by only 0.146(1) Å from it. The N–Cu distances are in the range normally observed for tetraaza macrocycle complexes, and the two N(imido)–Cu distances (1.937(2) Å) are shorter than the two N(amino)–Cu distances (2.026(2) Å), owing to the harder character of the donor atom and to the partial sp^2 character of the two nitrogen atoms related to the delocalization of the −1 charge on the oxygen atom of each amide. Observation of the crystal structure may suggest an apical interaction between the alkyne group and Cu^{2+}; however, the C(6)–Cu(1) and C(7)–Cu(1) distances are 2.805(4) and 2.737(4) Å, respectively, and suggest that the interaction between the metal center and the −C≡CH group is negligible. Moreover, IR spectra (KBr pellets) of solid samples of [**L1**Cu] and UV/Vis spectra (powder spread on paper) reveal a normal alkyne band (2108 cm^{-1}) and λ_{max} = 516 nm.

When the macrocyclic ligand $\mathbf{L2}H_2$ is taken into consideration, the distribution diagram (Figure 1B) shows that in this case the predominating species are the same as for $\mathbf{L1}H_2/Cu^{2+}$: the diprotonated ligand $[\mathbf{L2}H_4]^{2+}$ and the neutral square-planar complex [**L2**Cu]. Aside from the obvious macrocyclic effect exerted by the bis-deprotonated four-atom donor set in [**L2**Cu], even when the ligand is using only its two secondary amines, the −NH–$(CH_2)_3$–NH– group exerts a chelate effect. These two combined effects result in a higher stability constant for the metal-containing species, so that $[\mathbf{L2}H_4]^{2+}$ exists only up to pH 6 (instead of pH 7 in the case of $[\mathbf{L1}H_4]^{2+}$), and also higher percentages of complexes with nondeprotonated amides are allowed ($[\mathbf{L2}H_2Cu(OH)]^{+}$ reaches 65% at pH 5.3). The absorption spectrum of [**L2**Cu], measured at pH 8 (~100% of the neutral complex) displays the expected "pink" band, with λ_{max} = 512 nm (ε = 70 M^{-1} cm^{-1}), confirming the square-planar nature of this species (see Figure S3 in the Supporting Information for a UV/Vis spectrum recorded at pH 8.5).

In the case of the ligand $\mathbf{L3}H_2$, the amino groups are of the secondary type as in $\mathbf{L2}H_2$ but the system is acyclic. Moreover, the benzyl groups add bulkiness and lipophilicity to the vicinal amines and, as has already been noted in the previous section, this is reflected in the protonation constants. The same can be said of the complexation constants, which are ~1 log units lower than those for the open $\mathbf{L1}H_2$ ligand. However, the lower protonation and complexation constants balance each other to give a distribution diagram almost identical to that of $\mathbf{L1}H_2$: changing a primary amine into a secondary one (with a bulky substituent) in an acyclic ligand thus does not result in a significant change of the pH range of existence for the dominant species. Also, the in-plane coordination of the diamino-diimido donor set is not particularly affected by the presence of the benzyl substituents: [**L3**Cu] displays an absorption band with λ_{max} = 516 nm (ε = 76 M^{-1} cm^{-1}, see Figure S4 in the Supporting In-

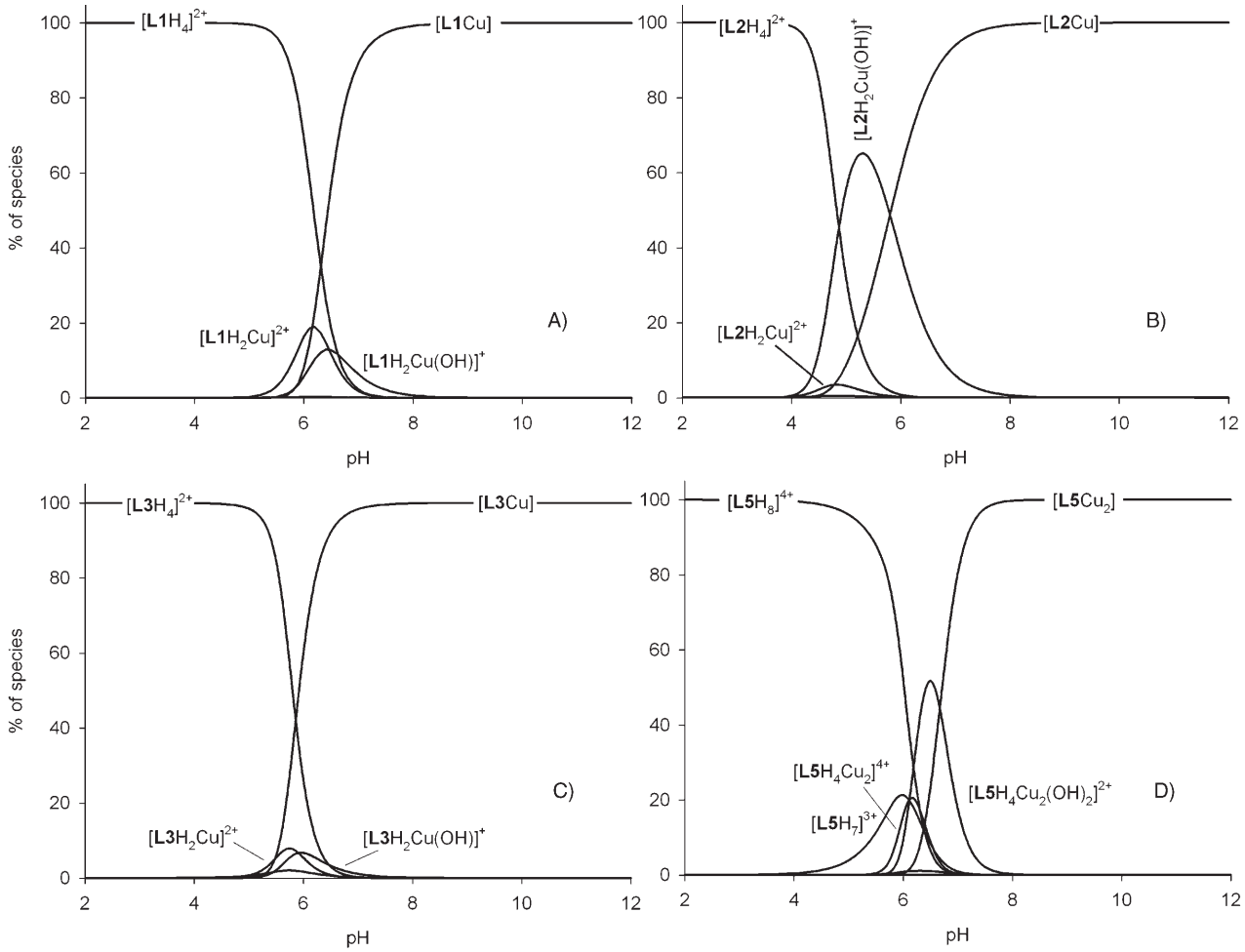

Figure 1. Distribution diagrams (% of species versus pH, water) for the systems: A) **L1**H_2/Cu^{2+} 1:1 molar ratio at a concentration of 10^{-3} M; B) **L2**H_2/Cu^{2+} 1:1 molar ratio at a concentration of 10^{-3} M; C) **L3**H_2/Cu^{2+} 1:1 molar ratio at a concentration of 10^{-3} M; and D) **L5**H_4/Cu^{2+} 1:2 molar ratio (10^{-3} M and 2×10^{-3} M, respectively). The protonation constants of the species not containing metal are reported in Table S1 in the Supporting Information. The formation constants of the metal-containing species and relative equilibria are reported in Table 1.

formation for a spectrum recorded at pH 8), indicating that the in-plane coordination is as efficient as that in [**L1**Cu].

Finally, the case of ligand **L5**H_4 should be taken into consideration. This molecule is cyclic and contains two 1,4,8,11-tetramine-5,7-dione units, meaning that it is capable of incorporating two Cu^{2+} ions. The four amino groups are of the secondary type, and are similar to those found in **L3**H_2 as regards the type and bulkiness of their substituents. The logarithmic formation constant of [**L5**H_4Cu_2]$^{4+}$, the complex in which the ligand is neutral and coordinates the two Cu^{2+} ions with its secondary amino groups, is roughly twice the logarithmic formation constant of [**L3**H_2Cu]$^{2+}$. For obvious geometric reasons, the two amino groups bound to the same aromatic ring cannot converge on the same Cu^{2+} ion, and the data also indicate that the ligand is too large and the distance between the two secondary amines belonging to the same tetraamino-dione framework is too long for a macrocyclic or chelate effect to be exerted. From the data listed in Table 1, log K for water deprotonation to give the resulting hydroxide complexes is calculated to be −5.91 for [**L5**H_4Cu(OH)]$^{+}$ and −12.23 for [**L5**H_4Cu$(OH)_2$]$^{2+}$. This indicates that the two hydroxide anions in the latter complex are probably not bridging the two coordinated Cu^{2+} ions, as this would result in a significantly easier water deprotonation process (for example, a pK_a value of 4.58 was found for water deprotonation in a bis-tren bis-Cu^{2+} cage complex, in which a bridging coordination mode was proposed for the hydroxide[12]). Finally, the deprotonation of the four amido groups and the coordination of the two Cu^{2+} ions is a more difficult process in the formation of [**L5**Cu_2], whose formation constant is significantly lower than double the formation constant of [**L3**Cu]. This is probably connected to the energy spent in rearranging the large macrocycle **L5**H_4 to give the double square-planar complex [**L5**Cu_2] and in the unfavorable geometry dictated by the *meta*-xylyl spacers that separate the two diamino-diimido donor sets. This latter effect is also reflected in the absorption band of [**L5**Cu_2], which is shifted towards longer wavelengths (λ_{max} = 527 nm, ε = 140 M^{-1} cm^{-1}, see Figure S5 in the Supporting Information for a spectrum measured at pH 11.0). As a result of the lower stability of the tetraamino tetraimido dimetallic complex, its formation starts and is completed at

about one unit of pH higher than in the $\mathbf{L3}H_2$ case (Figure 1D). However, the shape of the distribution diagram is similar to those found for all the non-translocating species. Only two species predominate in the 2–12 pH range: the one with the fully protonated amino groups $[\mathbf{L5}H_8]^{4+}$, and the one in which the amido protons are released and each Cu^{2+} is coordinated by a bis(amino)-bis(imido) donor set, the neutral $[\mathbf{L5}Cu_2]$.

Single and double cation translocation with molecular rearrangement: We and Fabbrizzi have demonstrated[6a] that pH-controlled single Ni^{2+} translocation takes place in a system with almost the same framework as $\mathbf{L4}H_2$, but with a benzyl group instead of propargyl. However, we also found[6c] that when Cu^{2+} is used inside the same ligand, an overall molecular rearrangement is obtained: $[\mathbf{L}H_2Cu]^{2+}$ is formed at $4.0 < pH < 6.0$, the Cu^{2+} ion is in the bis(aminoquinoline) compartment (trigonal-bipyramidal geometry, blue color, $\lambda_{max} = 616$ nm), and when the pH is raised above 6.0 the amido groups deprotonate. The diamino-diimido neutral complex [**L**Cu] is formed (prevalent at pH > 7.8, > 95% at pH 9.2) but its geometry is square-pyramidal, as indicated by the absorption band ($\lambda_{max} = 552$ nm). In this case, the chelate effect and tendency of Cu^{2+} to adopt five-coordination overwhelm the intrinsic square-planar geometry imposed by the diamino-diimido donor set in the bis-deprotonated 1,4,8,11-tetraamino-5,7-dione framework, and the system folds to allow coordination of one pyridine in the apical position with the Cu^{2+} center. These two complexes are depicted as **A1** and **A2** in Scheme 2. On the other hand, we and Fabbrizzi also found[7] that in a macrocyclic ligand that can be considered as a system containing two ligand units of the same kind, a neat cation translocation is also observed with Cu^{2+}: at $2.0 < pH < 6.1$ the $[\mathbf{L}H_4Cu_2]^{4+}$ complex is prevalent (each Cu^{2+} is trigonal-bipyramidal, blue color, $\lambda_{max} = 660$ nm, coordination sphere completed by water molecules), and at basic pH the cations are translocated with deprotonation of the amido groups to give the pink $[\mathbf{L}Cu_2]$ complex (prevalent at pH > 9.4, > 95% at pH > 10.2), in which each the Cu^{2+} center is authentically square-planar ($\lambda_{max} = 515$ nm). We put forward the hypothesis that the large benzyl groups were too bulky to allow folding of the entire macrocyclic framework for apical coordination of the pyridine groups. The two complexes are shown as **B1** and **B2** in Scheme 2.

On the basis of this information, we studied and compared the translocating properties of the ligands $\mathbf{L4}H_2$ and $\mathbf{L6}H_4$ towards Cu^{2+}. The solution behavior of the propargyl-substituted $\mathbf{L4}H_2$ ligand was studied by the usual potentiometric titration methods, using dioxane/water (4:1) as solvent. Figure 2 displays the distribution diagram for the 1:1 $\mathbf{L4}H_2/Cu^{2+}$ system and the visible spectra relative to the predominating species, from which it can be seen that translocation and rearrangement take place under pH control.

The $[\mathbf{L4}H_2Cu]^{2+}$ species is the complex in which the Cu^{2+} ion is coordinated by the neutral ligand with its two aminoquinoline bidentate units. This species is the prevalent one

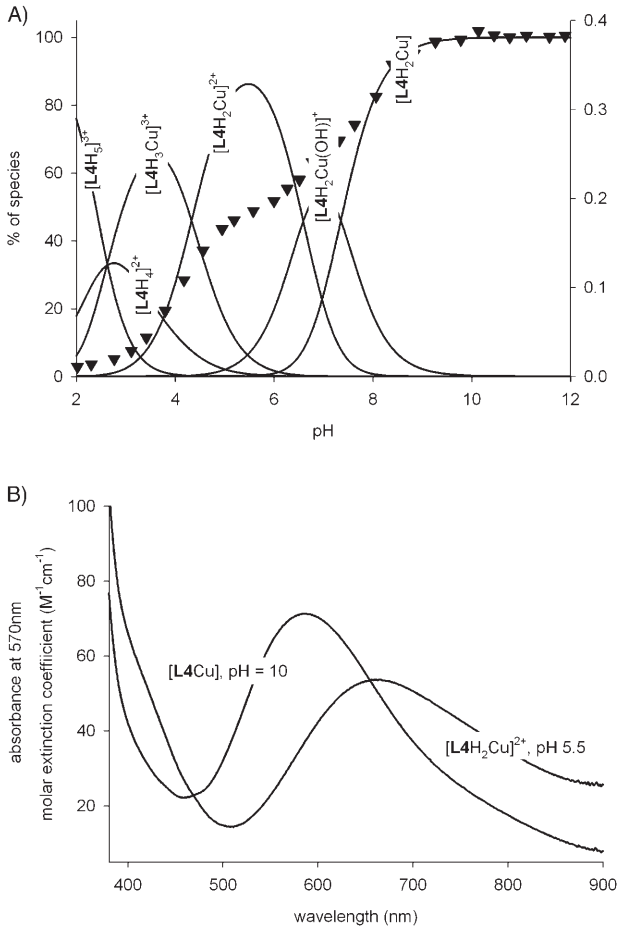

Figure 2. A) Distribution diagram (% of species versus pH) for the system $\mathbf{L4}H_2/Cu^{2+}$ 1:1 molar ratio at a concentration of 10^{-3} M (solid lines) in water/dioxane 1:4 v/v. The protonation constants of the species not containing metal are reported in Table S1 in the Supporting Information. The formation constants of the metal-containing species and relevant equilibria are: $[\mathbf{L4}H_3]^+ + Cu^{2+} \rightleftharpoons [\mathbf{L4}H_3Cu]^{3+}$, $\log K = 14.36(\pm 0.01)$; $\mathbf{L4}H_2 + Cu^{2+} \rightleftharpoons [\mathbf{L4}H_2Cu]^{2+}$, $\log K = 10.03(\pm 0.01)$; $\mathbf{L4}H_2 + Cu \rightleftharpoons [\mathbf{L4}H_2Cu(OH)]^+ + H^+$, $\log K = 3.44(\pm 0.01)$; $\mathbf{L4}H_2 + Cu^{2+} \rightleftharpoons [\mathbf{L4}Cu] + 2H^+$, $\log K = -3.91$. Black triangles are relative to the absorbance at 570 nm (i.e., at the maximum of absorption of [**L4**Cu]). The ascending value of this absorbance in the pH 4–7 range is due to the fact that the band relative to $[\mathbf{L4}H_2Cu]^{2+}$ has a non-negligible absorption at this wavelength (see also Figure 3B). B) Molar absorption spectra for $[\mathbf{L4}H_2Cu]^{2+}$ (recorded at pH 5.5) and for [**L4**Cu] (recorded at pH 10.0)

in solution at $4.5 < pH < 6.5$ reaching about 90% at pH 5.45, and it is indicated as **C1** in Scheme 3. Its absorption spectrum (recorded on a 10^{-3} M solution in both ligand and $[Cu(CF_3SO_3)_2]$, with pH set at 5.5 by microadditions of standard HNO_3; see Figure 2B) features an absorption maximum at 670 nm ($\varepsilon = 55\ M^{-1}\ cm^{-1}$). As has been reported in the literature for the analogous benzyl-substituted complex (**A1** in Scheme 2),[6c] this spectrum indicates that in $[\mathbf{L4}H_2Cu]^{2+}$ the copper cation is five-coordinate, and adopts a trigonal-bipyramidal geometry in which the fifth coordination position is occupied by a water molecule. Water deprotonation is observed on raising the pH above 6, with $[\mathbf{L4}H_2Cu(OH)]^+$ reaching its maximum (55%) at pH 7.0 ($pK_a = 6.59$). Further increase in pH causes the two amido protons to be re-

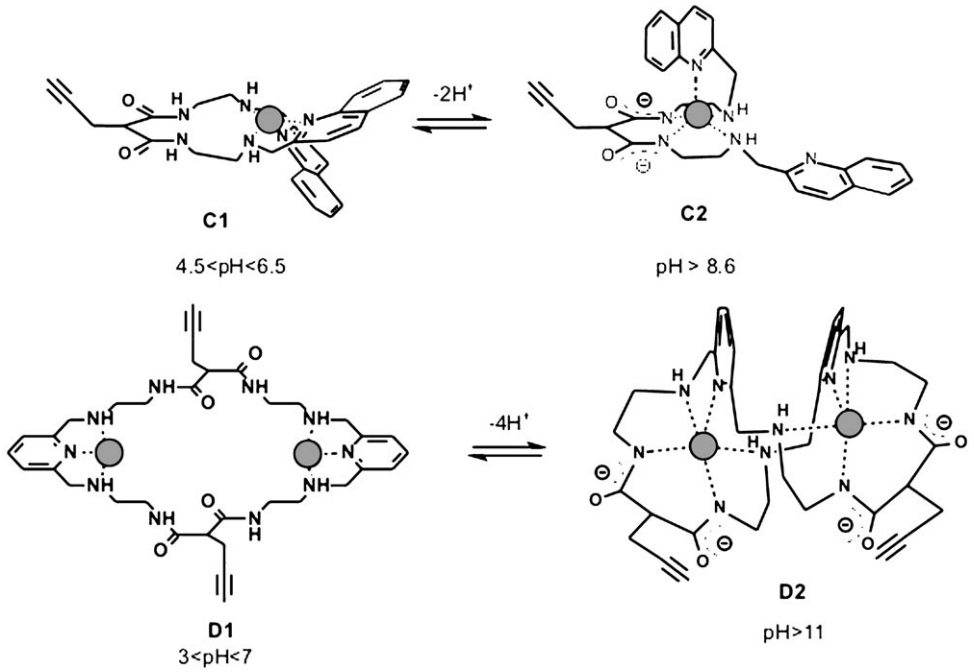

Scheme 3. Scheme for the pH-driven translocation plus rearrangement of one or two Cu^{2+} ions.

leased and the Cu^{2+} ion to translocate inside the diamino-diimido compartment, leading to the formation of the neutral [**L4**Cu] complex in above 95% yield at pH > 8.6. Accordingly, translocation of the Cu^{2+} ion takes place on changing the pH from 5 to 9, for example, or vice versa. However, in this complex, the Cu^{2+} ion is not square-planar: its visible absorption (recorded on a 10^{-3} M solution in both ligand and $[Cu(CF_3SO_3)_2]$, with pH set at 10.0 by microadditions of standard KOH; see Figure 2B) is centered at $\lambda_{max} = 570$ nm ($\varepsilon = 78\,M^{-1}\,cm^{-1}$), indicating apical coordination of one of the quinoline groups to the Cu^{2+} center and the displacement of the copper cation from the plane formed by the four nitrogen atoms of the diamino-diimido donor set, as was observed for Cu^{2+} with the analogous benzyl-containing ligand (Scheme 2, form **A2**). The [**L4**Cu] complex can thus be assigned to be **C2** (see Scheme 3) and according to the scheme, translocation of the copper cation takes place under pH control. However it also involves a more complicated overall molecular rearrangement: Cu^{2+} does not simply change coordinative compartments because one quinoline group always remains bound to it. Figure 2A also shows (black triangles) the profile of the absorption at 570 nm versus pH, which superimposes nicely with the formation profile of its parent species [**L4**Cu].

Notably, in this translocating system, deprotonation of the amide groups and coordination of Cu^{2+} by the diamino-diimido donor set takes place at a pH remarkably higher than in the non-translocating systems. For example, in the system with $\mathbf{L3}H_2/Cu^{2+}$ in a 1:1 molar ratio, [**L3**Cu] is present at more than 95% at pH 7, whereas to attain the same percentage for [**L4**Cu] requires pH 8.6. This difference is due to the competitive effect of the two chelating aminoquinoline units, that is, to the formation of the stable $[\mathbf{L4}H_2Cu]^{2+}$ complex. As discussed in the previous section, competition of the related species in the case of $\mathbf{L3}H_2$ is negligible because $[\mathbf{L3}H_2Cu]^{2+}$ is not very stable.

Quite surprisingly, *double Cu^{2+} translocation with rearrangement* can also be observed on changing the pH for the system made of $\mathbf{L6}H_4/Cu^{2+}$ in a 1:2 molar ratio. For this system, potentiometric titrations carried out in water allowed us to determine the formation constants and the distribution diagram (Figure 3A; see caption for the log$K$ values and the formation equilibria involved) of the species present in solution as a function of pH. The important species involved in the translocation process are $[\mathbf{L6}H_4Cu_2]^{4+}$ and $[\mathbf{L6}Cu_2]$. $[\mathbf{L6}H_4Cu_2]^{4+}$ is the species in which the ligand is in its neutral form, and coordinates two Cu^{2+} ions, each one with the tridentate chelating diaminopyridine units; it is indicated as **D1** in Scheme 3. This species has a blue color and displays an absorption spectrum with $\lambda_{max} = 660$ nm ($\varepsilon = 128\,M^{-1}\,cm^{-1}$; see Figure 3B), typical of pentacoordinate trigonal-bipyramidal Cu^{2+} (the remaining two coordinating positions are occupied by water molecules), similar to what we and Fabbrizzi have previously found[7] with the benzyl-substituted analogue ligand (**B1** in Scheme 2). This $2\,Cu^{2+}$/neutral ligand species is prevalent in the $2.6 < pH < 4.9$ interval, reaching its maximum (93%) at pH 3.5. This is different from what was found for the *meta*-xylyl analogue $\mathbf{L5}H_4$: in that case, the absence of the pyridine nitrogen atom does not allow any kind of chelating effect; thus, the $[\mathbf{L5}H_4Cu_2]^{4+}$ species is not very stable. The corresponding logarithmic formation constants, 11.39 for $[\mathbf{L5}H_4Cu_2]^{4+}$ and 25.31 for $[\mathbf{L6}H_4Cu_2]^{4+}$, can be directly compared and reflect this difference.

The high stability of the Cu^{2+}-diaminopyridine moiety is also reflected in the existence of the hydroxide-coordinated species $[\mathbf{L6}H_4Cu_2(OH)]^{3+}$ and $[\mathbf{L6}H_4Cu_2(OH)_2]^{2+}$, which are prevalent up to pH 9.1, and in which the Cu^{2+} ions are still in the diaminopyridine tridentate compartments. The pK_a values of only 4.84 and 7.49 calculated for the first and second deprotonation of water indicate that at least one of the OH^- ions is probably bridging between the two copper cations, in accord with the previously demonstrated capability of the very similar complex **B1** to bind a variety of bridging anions.[7] In the visible absorption spectra, these species display almost no shift of the absorption bands relative to **D1** (see Figure 3B). As a consequence of the stability of the Cu^{2+}-diaminopyridine moiety, the deprotonation of the amido groups and the translocation of the Cu^{2+} ions with

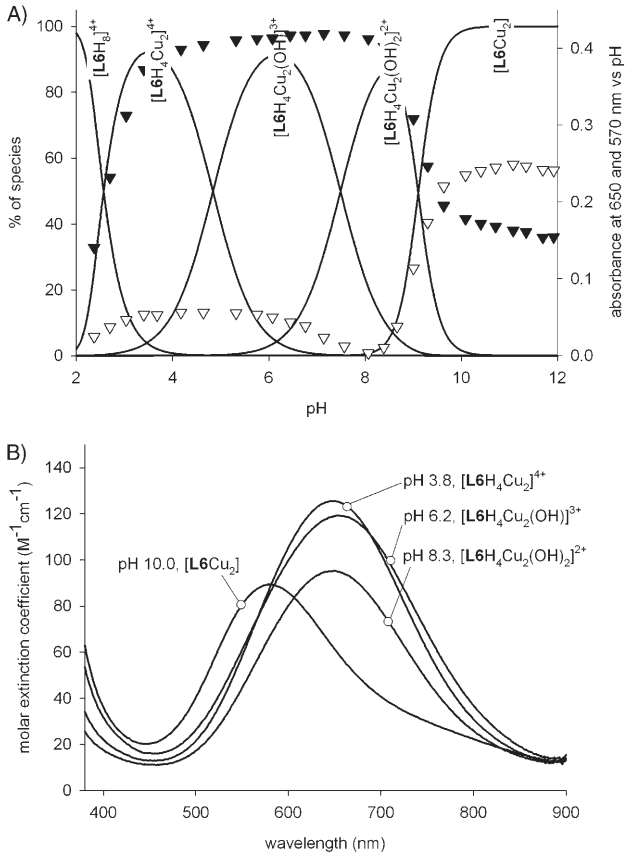

Figure 3. A) Solid lines represent the % of species versus pH for the species existing in the pH 2–12 range for the system comprising 10^{-3} M **L6**H_4 and 2×10^{-3} M Cu^{2+} (i.e., 1:2 molar ratio). The protonation constants of the species not containing metal are reported in Table S1 in the Supporting Information. The formation constants of the metal-containing species, with relevant equilibria are: **L6**$H_4+2Cu^{2+}\rightleftharpoons[$**L6**$H_4Cu_2]^{4+}$, log$K$ = 25.31; **L6**$H_4+2Cu^{2+}\rightleftharpoons[$**L6**$H_4Cu_2(OH)]^{3+}+H^+$, log$K$ = 20.47; **L6**$H_4+2Cu^{2+}\rightleftharpoons[$**L6**$H_4Cu_2(OH)_2]^{2+}+2H^+$, log$K$ = 12.98; **L6**$H_4+2Cu^{2+}\rightleftharpoons[$**L6**$Cu_2]+4H^+$, log$K$ = −5.23. White triangles represent the absorbance versus pH measured at 570 nm, λ_{max} for the [**L6**Cu_2] species. The slight absorbance increase in the $2<$pH<8 region is due to the fact that $[$**L6**$H_4Cu_2]^{4+}$ (and its hydroxide complexes) also has a non-negligible absorbance at this wavelength. Black triangles represent the absorbance versus pH measured at 650 nm, λ_{max} for the $[$**L6**$H_4Cu_2]^{4+}$ species; in this case the residual absorbance observed at pH>8 is also due to the fact that [**L6**Cu_2] has a non-negligible absorbance at this wavelength. B) Absorption spectra for $[$**L6**$H_4Cu_2]^{4+}$, $[$**L6**$H_4Cu_2(OH)]^{3+}$, $[$**L6**$H_4Cu_2(OH)_2]^{2+}$, and [**L6**Cu_2], measured at various pH values (at which the relative species reaches its maximum percentage).

formation of the diamino-diimido neutral complex [**L6**Cu_2] (**D2** in Scheme 3) is pushed to a very basic zone. This complex begins to form at pH>8.1 and reaches $>95\%$ at pH 9.8, while the corresponding species for the non-translocating ligand **L5**H_4 (i.e., [**L5**Cu_2]) begins to form at pH 6.0 and goes over 95% at pH 7.7. Owing to the very effective chelating action of the diaminopyridine units in the large macrocyclic system **L6**H_4, the formation of the diamino-diimido complex is even more difficult than in the single-translocating **L4**H_2 ligand, in which simple bidentate units chelate the Cu^{2+} ion.

Even if [**L6**Cu_2] has the same formulation as species **B2** in Scheme 2, its absorption spectrum strongly indicates that its geometry is different. In particular, it has a visible spectrum with λ_{max} = 575 nm (ε = 90 $M^{-1}cm^{-1}$; see Figure 3B), which is thus centered at too long a wavelength maximum for even a distorted square-planar arrangement of the diamino-diimido donor set. Accordingly, each Cu^{2+} should be pentacoordinate and square-pyramidal, as has been found in the cases of **A2** and **C2**. Thus, the unusual geometrical arrangement of [**L6**Cu_2] can be hypothesized as **D2** in Scheme 3: on changing pH from 4 to 10, for example, the whole molecular system rearranges and folds with translocation, allowing each pyridine unit to apically coordinate one Cu^{2+} ion. As expected, plotting the absorbance versus pH taken at λ_{max} both for [**L6**Cu_2] and $[$**L6**$H_4Cu_2]^{4+}$ results in profiles that superimpose correctly on the distribution curves of the relative species (Figure 3A, black and white triangles).

Translocation plus folding is indeed confirmed by the crystal and molecular structure determined by X-ray diffraction of a single crystal of [**L6**Cu_2] (Figure 4). Each Cu^{2+} ion lies outside of the plane defined by the diamino-diimido donor set by 0.341(5) Å for Cu(1) and 0.322(6) Å for Cu(2), and both metal centers are coordinated apically by one pyridine, with Cu–N distances (2.264(9) Å for Cu(1) and 2.288(10) Å for Cu(2)) that confirm the interaction with the apical N atoms. Therefore each metal center is pentacoordinate and has a distorted square-pyramidal geometry.

Quite interestingly, translocation plus folding is allowed in the systems coordinating one single Cu^{2+} ion (see **A1** and **A2** in Scheme 2 and **C1** and **C2** in Scheme 3), independent of the nature of the substituent between the C=O groups (i.e., benzyl or propargyl): molecular modeling (Hyperchem

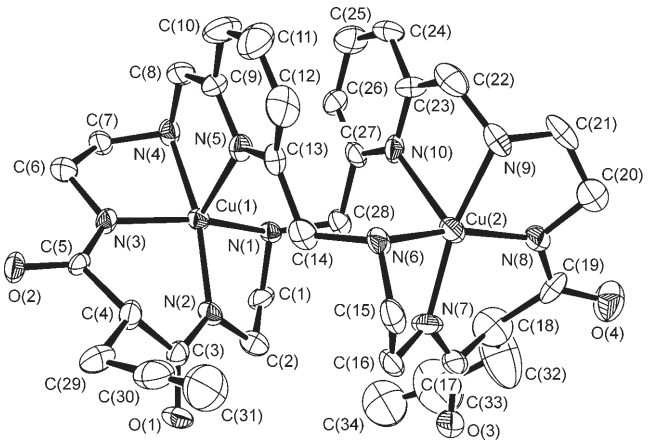

Figure 4. Structure of the [**L6**Cu_2] complex (ORTEP view, ellipsoids are drawn at the 30% probability level, hydrogen atoms and solvent water molecules omitted for clarity). Both metal centers exhibit a distorted square-pyramidal coordination sphere. Selected bond lengths [Å] and angles [°]: Cu(1)–N(1) 2.032(9), Cu(1)–N(2) 1.937(10), Cu(1)–N(3) 1.943(10), Cu(1)–N(4) 2.052(10), Cu(1)–N(5) 2.264(9), Cu(2)–N(6) 2.063(10), Cu(2)–N(7) 1.929(11), Cu(2)–N(8) 1.964(11), Cu(2)–N(9) 2.055(10), Cu(2)–N(10) 2.288(10); N(1)-Cu(1)-N(2) 84.08(39), N(1)-Cu(1)-N(4) 94.91(37), N(1)-Cu(1)-N(5) 105.38(35), N(2)-Cu(1)-N(3) 92.12(41), N(2)-Cu(1)-N(5) 115.55(41), N(3)-Cu(1)-N(4) 82.36(38), N(3)-Cu(1)-N(5) 97.07(39), N(4)-Cu(1)-N(5) 80.45(40), N(6)-Cu(2)-N(7) 81.62(51), N(6)-Cu(2)-N(9) 95.19(43), N(6)-Cu(2)-N(10) 95.55(37), N(7)-Cu(2)-N(8) 93.22(51), N(7)-Cu(2)-N(10) 118.01(42), N(8)-Cu(2)-N(9) 84.07(45), N(8)-Cu(2)-N(10) 104.40(41), N(9)-Cu(2)-N(10) 78.44(44).

6.0 package) suggests that on coordination of one pyridine group, the benzyl or propargyl substituent is on the other side of the plane (defined by the four nitrogen donors) from the coordinating heterocycle, with no reciprocal interaction. Different behavior is found for the larger macrocyclic systems in which double cation translocation takes place. With the bulky benzyl substituent, folding is not allowed and true square-planar coordination is found for each Cu^{2+} ion (**B2**, Scheme 2), whereas the slim $-CH_2-C\equiv CH$ fragment allows folding, apical coordination of the pyridines, and consequently molecular folding with translocation. The dimensions of the substituent between the two C=O groups are crucial. In the crystal structure of [**L6**Cu_2], each $-CH_2-C\equiv CH$ group is folded away with respect to the plane of the diamino-diimido donor set binding to the closest metal center, and the terminal alkyne carbon atom is near the $-CH_2-CH_2-$ moiety that connects the $-NH-$ and $-N^{-}-$ groups in the 1,4 positions of the other diamino-diimido framework. Bond lengths as short as 2.61(5) Å for the C(34) proton and one proton of C(1) and 2.75(2) Å for the C(31) proton and one proton of C(15) may be calculated for the two terminal alkyne carbons: substituting the $-C\equiv CH$ group with a benzene ring would thus result in serious steric crowding between the $-CH_2-CH_2-$ chains and the benzyl protons.

Crystal and molecular structure of [L6Cu$_2$]: The crystal and molecular structure of the Cu^{2+} complex as hydrate crystals [**L6**Cu_2]·9H_2O has been obtained from an X-ray diffraction study and is shown in Figure 4. The N(imido)–Cu distances are 1.944(10) Å (av) and the N(amino)–Cu distances 2.050(11) Å (av). Delocalization of the negative charge of the N(imido) atoms over the carboxyl groups makes the N(imido)–C(carboxy) distance, 1.293(10) Å (average), significantly shorter than the other N–C bond lengths (1.472(5) Å, average). The [**L6**Cu_2] complex shows the four N atoms of each diamino-diimido donor set to be almost coplanar: the mean deviation from the N_4 best plane are 0.06(1) Å for N(1)-N(2)-N(3)-N(4) and 0.04(1) Å for N(6)-N(7)-N(8)-N(9). However, the two metal centers are significantly out of the amine best planes by 0.341(5) Å for Cu(1) and 0.322(6) Å for Cu(2). The distances to the apical N(pyridine) atoms are 2.264(9) for Cu(1) and 2.288(10) Å for Cu(2) and are in agreement with that already found for an axial N(pyridine) donor atom.[10] The metal centers are definitely pentacoordinate and have a distorted square-pyramidal geometry, the apical N(pyridine) atoms being far away from the normal to the plane of the basal donor set. The molecular folding of the [**L6**]$^{4-}$ ligand, which allows pentacoordination for the two metal centers, places the two pyridine rings at a distance that is compatible with weak face-to-face π-stacking interactions; the centroid–centroid separation is 3.60(2) Å and the shorter interatomic distances are between N(5) and C(27) (3.14(1) Å) and between N(10) and C(13) (3.20(1) Å). Finally, various hydrogen-bonding interactions occur: the O(2), O(3), and O(4) carboxy-oxygen atoms of the [**L6**Cu_2] complex are proton acceptors in O–H···O interactions with water molecules. The quality of the [**L6**Cu_2] crystal did not allow us to define the positions of all the water protons, and only the O(water)···O(carboxy) donor–acceptor distances can be clearly defined; they range between 2.67(2) and 3.04(2) Å. Also the N(6) and N(9) secondary amines are proton donors for water molecules and the N–H···O(water) features are: N···O 2.97(2)–3.172(2) Å, H···O 2.10(2)–2.42(2) Å, N–H···O 159(1)–139(1)°. The other two secondary amines, N(1) and N(4), are proton donors for the O(1) carboxy-oxygen atom of an adjacent molecule. The N–H···O(carboxy) interactions have the following features: N···O 3.00(1)–3.05(1) Å, H···O 2.09(1)–2.17(1) Å, N–H···O 171(1)–162(1)°, and produce an infinite chain of [**L6**Cu_2] complexes that extends along the *b* crystallographic axis.

Electrochemical oxidation of Cu^{2+} centers to Cu^{3+}: The electrochemical properties of the Cu^{2+} complexes of ligands **L1**H_2–**L6**H_4 were examined in water (water/dioxane 1:4 in the case of **L4**H_2), by means of cyclic voltammetry experiments. Measurements carried out on solutions prepared by simply mixing free ligand and [$Cu(CF_3SO_3)_2$] in 1:1 (**L1**H_2–**L4**H_2) or 1:2 (**L5**H_4 and **L6**H_4) molar ratios resulted in flat profiles, indicating that no oxidation took place in the potential window examined (from −500 to +1500 mV versus SCE). To observe the appearance of an oxidation wave (Cu^{3+}/Cu^{2+} couple) it was necessary to add enough standard KOH to deprotonate the amido groups and reach pH values at which, according to the distribution diagrams, the neutral Cu^{2+}–amino-imido complexes are formed at >95%. This behavior is expected, because oxidation of Cu^{2+} to Cu^{3+} is not observed (at least in the electrochemical window allowed in water) in the complexes formed by Cu^{2+} with amino/heterocycle ligands, while it is known[3] that it can reversibly take place when Cu^{2+} is coordinated by the diamino-diimido donor set of the deprotonated 1,4,8,11-tetraamino-5,7-dione framework. Figure 5A displays the CV profile obtained for **L1**H_2 + Cu^{2+} at pH 8.0, at which value [**L1**Cu] is formed in 99% yield. The CV profile is reversible, with $E_{1/2}$ = 755 mV versus SCE (ΔE = 140 mV). This value compares well with those previously reported for the analogous [**L**Cu] complexes with open ligands **L**H_2 (Scheme 1A, left) either 1,4,8,11-tetraaza-5,7-dione (R = H in Scheme 1A, left, $E_{1/2}$ = 700 mV versus SCE) or 6-benzyl-1,4,8,11-tetraaza-5,7-dione (R = benzyl in Scheme 1A, left, $E_{1/2}$ = 740 mV versus SCE).[10] Similar behavior is found for **L2**H_2, with a reversible CV profile with full current intensity found at pH 7.8, with [**L2**Cu] formed at about 99% yield. However Cu^{2+} is oxidized to Cu^{3+} at a lower potential (657 mV versus SCE), as expected from the macrocyclic stabilization effect on high oxidation states of the encircled metal.[3c]

Ligands **L3**H_2–**L6**H_4 have the common feature of having secondary amino groups with large CH_2-phenyl or CH_2-pyridyl substituents. This has a dramatic effect on the oxidation process. In the case of [**L3**Cu], no pyridine is contained in the ligand framework; the complex is square-planar (λ_{max} = 516 nm), but in the CV profile only an oxidation wave is observed, with no reduction. The peak potential is about 900 mV versus SCE. This value is compatible with the po-

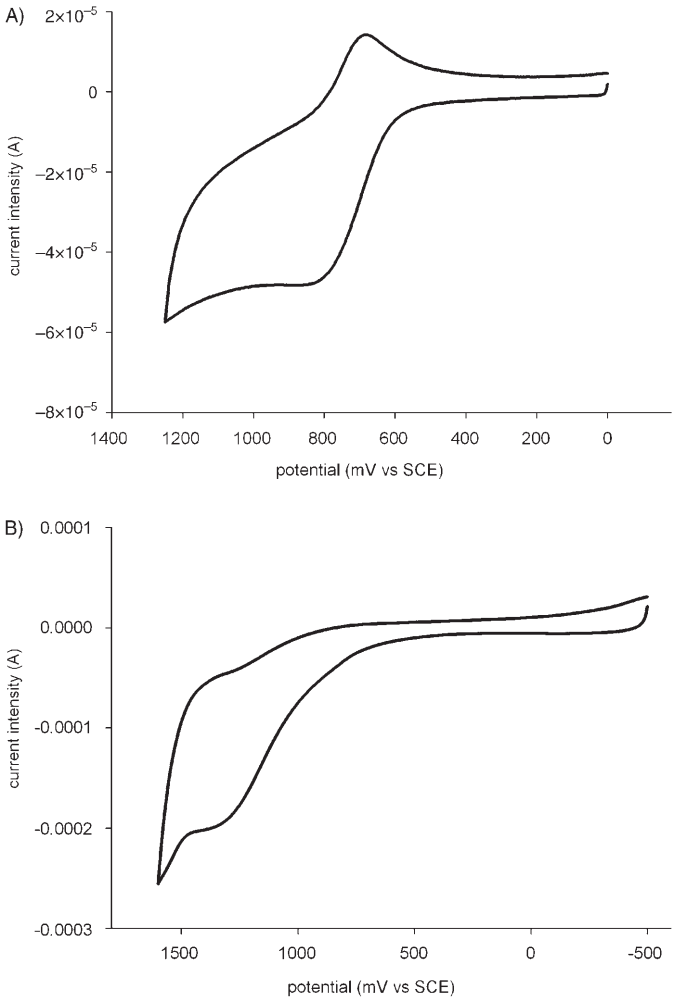

Figure 5. Cyclic voltammetry profiles obtained in water (0.1 M KNO_3) for A) [**L1**Cu] at pH 8.0 and B) [**L6**Cu_2] at pH 10.2. Scan rate = 200 mV s^{-1}.

tential values observed for the oxidation peaks of [**L1**Cu] and [**L2**Cu], and is consistent with the observation that in the amino-imido complexes of Cu^{2+}, the oxidation potential of the Cu^{3+}/Cu^{2+} couple is directly proportional to the maximum of the d–d absorption band.[13] As regards the nonreversible profile observed, the hypothesis may be put forward that the large benzyl groups cause unfavorable steric crowding in the complex of the small Cu^{3+} ion, which is d^8, low-spin, and square-planar,[3c] and is stabilized in particular by diamino-diimido donor sets capable of tightly encircling the metal cation.[14] Moreover, decomposition of Cu^{3+} complexes inside amino-imido ligands has been proposed to occur through base-promoted deprotonation of an amine group and the formation of a transient N=C double bond.[14,15] This may be favored in our ligands by conjugation with the aromatic ring.

When the [**L5**Cu_2] complex is taken into consideration, not even an irreversible oxidation wave is observed before water discharge. Indeed, this may be expected considering that the [**L5**Cu_2] complex absorbs at 527 nm, indicating significant distortion from perfect square-planar coordination of the Cu^{2+} ions, which shifts the oxidation potential outside the potential window allowed by the solvent (water).[13]

Finally, when the imino-imido complexes of the translocating systems [**L4**Cu] and [**L6**Cu_2] are taken into consideration, similar behavior is found. Irreversible oxidation is observed near the solvent discharge (~1300 mV versus SCE. See Figure 5B for the case of [**L6**Cu_2]; pH 10.2) Axial coordination in Cu^{2+} diamino-diimido complexes has been shown to favor oxidation to Cu^{3+},[3c] but at the same time, in our complexes this imparts such a displacement of the Cu^{2+} ion from the N_4 plane that the two effects balance in a shift of the oxidation potential near the anodic limit of solvent discharge. Moreover, irreversibility must take into account both the promotion of decomposition pathways of the Cu^{3+} complex (that should be more significant at the particularly basic pH necessary to form the deprotonated complexes in these two ligands) and the ligand rearrangements following oxidation, as the d^8 Cu^{3+} ion is square planar and, consequently, the square-pyramidal arrangement shown in Figure 5, for example, must be disrupted.

Conclusion

Some general conclusions about the behavior of the 1,4,8,11-tetraamino-5,7-dione framework either as a simple ligand for Cu^{2+} or inside translocating systems for Cu^{2+} may be drawn from this work, based on a set of new ligands containing this framework and a propargyl moiety as the substituent on the C atom between C=O groups. In non-translocating systems (**L1**H_2–**L3**H_2 and **L5**H_4), the propargyl group facilitates the solubilization of ligands and complexes in water, but does not have any additional effect on Cu^{2+} complexation. Also the incorporation of secondary amine groups does not lead to significant differences in the complexation properties of these ligands, in particular with respect to the pH of formation of the neutral complexes with deprotonated amido groups. However, the maximum of the d–d absorption band is significantly shifted towards longer wavelengths when the substituent on the secondary amines is bulky and two tetraaminodione units are included in a macrocyclic framework, which reflects hindered access to perfect square-planar coordination of the Cu^{2+} ion in the complexes. The effect of secondary amines is dramatic on the oxidation of the complexed Cu^{2+} ion to Cu^{3+}: with the exception of the [**L2**Cu] complex of the macrocyclic ligand **L2**H_2, which profits from the macrocyclic effect and displays a reversible oxidation at a potential lower than [**L1**Cu], equipping the amine with bulky groups such as benzyl prevents reversibility. Moreover, inclusion of the ligand with secondary bulky substituents in a large macrocyclic framework (**L5**H_4) pushes the irreversible oxidation process out of the water electrochemical window. When systems in which cation translocation can take place are examined, the role of the substituent on the carbon atom between the two C=O groups is negligible in open ligands. Owing to the flexibility of the ligand framework, the folding of a methyl-het-

erocycle arm always follows translocation of Cu^{2+} from the amino-heterocycle compartment to the diamino-diimido one. A square-pyramidal coordination geometry is obtained for Cu^{2+} in [**L4**Cu] as in its analogues with bulkier substituents instead of propargyl. On the other hand, the dimensions of the substituent are critical when large, cyclic, double-translocating systems like [**L6**H_4] are taken into consideration. The slim propargyl group allows folding of the ligand framework to follow translocation from the diamino-pyridine compartments to the diamino-diimido ones, so that apical coordination of the pyridine to Cu^{2+} and square-pyramidal coordination are obtained in the [**L6**Cu_2] complex, while in the same ligand with benzyl instead of propargyl, folding is prevented by the bulkiness of the substituent, and truly square-planar Cu^{2+} is obtained. Finally, the electrochemical oxidation of Cu^{2+} to Cu^{3+} is made irreversible by apical coordination of a heterocycle in the diamino-diimido complexes, and the oxidation peak is pushed close to the limits of the water electrochemical window.

Experimental Section

Syntheses: Benzaldehyde, 2-quinoline carboxaldehyde, isophtalaldehyde, and 2,6-pyridine dicarboxaldehyde were purchased from Aldrich or Fluka, and used as supplied. 2-Propargyldiethyl malonate was prepared according to reference [16], and the crude yellow oil was further purified by distillation under reduced pressure through a microdistillation apparatus fitted with a short Vigreux column, (b.p. 51 °C at 5×10^{-2} mbar), resulting in a colorless oil. 1,3-(2′-Aminoethylamino)propane was prepared according to reference [17].

***N,N′*-Bis-(2-aminoethyl)-2-prop-2-ynylmalonamide (L1H_2)**: 2-Propargyldiethyl malonate (15.0 g, 75.7 mmol) was dissolved in a large excess of ethylenediamine, previously distilled from CaH_2. The mixture was stirred under nitrogen at room temperature for a week. The ethylenediamine was evaporated under vacuum and the crude white product was repeatedly washed with diethyl ether, resulting in a white powder that was dried under vacuum (84% yield). ^{1}H NMR ($CDCl_3$): δ = 7.7 (br; CO-NH-), 3.4 (m, 5H; CO-CH(R)-CO + CO-NH-CH_2), 2.8 (m, 6H; C≡C-CH_2- + -CH_2-NH_2), 2.12 ppm (s, 1H; *H*C≡C-); MS (ESI): *m*/*z*: 227 [**L1**H_2+H^+]; elemental analysis calcd (%) for $C_{10}H_{18}N_4O_2$: C 53.08, H 8.02, N 24.75; found: C 53.01, H 8.08, N 24.72.

6-Prop-2-ynyl-1,4,8,11-tetraazacyclotetradecane-5,7-dione (L2H_2): 2-Propargyldiethyl malonate (10.0 g, 50.5 mmol) and 1,3-(2′-aminoethylamino)propane (8.0 g, 0.05 mmol) were dissolved in anhydrous ethanol (100 mL). The mixture was refluxed for three days under nitrogen. After the mixture was allowed to cool to room temperature, the solvent was concentrated on a rotary evaporator and the mixture was left standing at 0 °C until a yellow precipitate formed. The product was collected by filtration and washed with chilled ethanol (2×5 mL) and diethyl ether (2×10 mL), to yield a white solid (20%). ^{1}H NMR ($CDCl_3$): δ = 7.8 (br, 2H; CO-NH-), 3.4–3.5 (m, 5H; CO-CH(R)-CO + CO-NH-CH_2), 2.7–2.8 (m, 10H; C≡C-CH_2- + -CH_2-NH-CH_2), 2.08 (s, 1H; HC≡C-), 1.68 ppm (t, 2H; -CH_2-CH_2-CH_2-); MS (ESI): *m*/*z*: 267 [**L2**H_2+H^+]; elemental analysis calcd (%) for $C_{13}H_{22}N_4O_2$: C 58.62, H 8.32 N 21.02; found: C 58.59, H 8.35, N 20.99.

***N,N′*-Bis-(2-benzylaminoethyl)-2-prop-2-ynylmalonamide (L3H_2)**: A solution of **L1**H_2 (0.453 g, 2 mmol) in methanol (20 mL) was added dropwise to a solution of benzaldehyde (0.410 g, 4.0 mmol) in methanol (30 mL) at room temperature. After one night the mixture was reduced in situ with an excess of $NaBH_4$ (added in portions as a solid at room temperature) and further refluxed for 2 h. The solvent was then evaporated under vacuum, and the crude product was treated with KOH (0.1 M, 50 mL) and extracted with dichloromethane (3×50 mL). The combined organic phases were dried over Na_2SO_4 and filtered. Evaporation of the solvent on a rotary evaporator gave the product as a white solid in 87% yield. ^{1}H NMR ($CDCl_3$): δ = 7.1–7.2 (m, 10H; H of the benzene rings), 3.80 (s, 4H; NH-CH_2-benzene), 3.2–3.5 (m, 5H; CO-CH(R)-CO + CO-NH-CH_2), 2.74–2.76 (m, 6H; C≡C-CH_2- + -CH_2-NH-CH_2-benzene), 1.9–2.0 ppm (br; HC≡C- + amine protons); MS (ESI): *m*/*z*: 407 [**L3**H_2+H^+]; elemental analysis calcd (%) for $C_{24}H_{30}N_4O_2$: C 70.91, H 7.44, N 13.77; found: C 70.93, H 7.46, N 13.74.

2-Prop-2-ynyl-*N,N′*-bis-{2-[(quinolin-2-ylmethyl)amino]ethyl}malonamide (L4H_2): The ligand was prepared by the same procedure used for **L3**H_2, using ethanol as solvent, starting with **L1**H_2 (0.452 g, 2.0 mmol) and 2-quinoline carboxyaldehyde(0.628 g, 4.0 mmol). The product was obtained in 82.6% yield as a yellowish solid. ^{1}H NMR ($CDCl_3$): δ = 8.12 (d, 2H), 8.03 (d, 2H), 7.76 (d, 2H), 7.70 (t, 2H), 7.51 (t, 2H), 7.36 (d, 2H; H of the quinoline rings), 4.02 (s, 4H; NH-CH_2-quinoline), 3.2–3.5 (m, 5H, CO-CH(R)-CO + CO-NH-CH_2), 2.8–2.9 (m, 6H, C≡C-CH_2- + -CH_2-NH-CH_2-quinoline), 2.0 ppm (s, HC≡C-); MS (ESI): *m*/*z*: 509 [**L4**H_2+H^+]; elemental analysis calcd (%) for $C_{31}H_{36}N_6O_3Cl_2$ (**L4**H_2·H_2O·CH_2Cl_2): C 60.88, H 5.93, N 13.73; found: C 60.85, H 5.95, N 13.70.

8,26-Diprop-2-ynyl-3,6,10,13,21,24,28,31-octaazatricyclo[31.3.1.1*15,19*]-octatriaconta-1(36),15,17,19(38),33(37),34-hexaene-7,9,25,27-tetraone (L5H_4): A solution of **L1**H_2 (226 mg, 1 mmol) in acetonitrile (40 mL) and methanol (5 mL) was added dropwise to a solution of isophtalaldehyde (134 mg, 1 mmol) in acetonitrile (60 mL) at room temperature. A white precipitate immediately began to form and the mixture was further stirred overnight. The white solid was collected by suction filtration, redissolved in methanol (60 mL) and treated at room temperature with excess $NaBH_4$ (added in portions as a solid). The mixture was then kept at reflux overnight, the solvent was removed on a rotary evaporator, and the solid product mixture was treated with KOH (0.1 M, 50 mL). The aqueous solution obtained was extracted with $CHCl_3$ (3×50 mL) and the organic portions were gathered and dried over Na_2SO_4. After filtration, chloroform was removed on a rotary evaporator, to leave the product as a white solid in 86% yield. ^{1}H NMR ($CDCl_3$): δ = 7.68 (t, 4H; CO-N*H*-CH_2); 7.44 (s, 2H; benzene H), 7.25 (t, 2H; benzene H), 7.12 (d, 4H; benzene H), 3.79 (s, 8H; NH-CH_2-arene), 3.3–3.4 (m, 10H; CO-CH(R)-CO + CO-NH-CH_2), 2.7–2.8 (m, 12H; C≡C-CH_2- + -CH_2-NH-CH_2), 1.8–1.9 ppm (br; HC≡C- + amine protons); MS (ESI): *m*/*z*: 657 [**L5**H_4+H^+]; elemental analysis calcd (%) for $C_{36}H_{48}N_8O_4$: C 65.83, H 7.36, N 17.05; found: C 65.80, H 7.38, N 17.01.

8,26-Diprop-2-ynyl-3,6,10,13,21,24,28,31,37,38-decaazatricyclo-[31.3.1.1*15,19*]octatriaconta-1(36),15,17,19(38),33(37),34-hexaene-7,9,25,27-tetraone (L6H_4): Ligand **L6**H_4 was prepared by the same procedure used for **L5**H_4, by reacting **L1**H_2 (226 mg, 1 mmol) with pyridine-2,6-dicarbaldehyde (135 mg, 1 mmol) to yield the product in 84% yield. ^{1}H NMR ($CDCl_3$): δ = 7.90 (t, 4H; CO-N*H*-CH_2), 7.65 (t, 2H; pyridine H), 7.18 (d, 4H; pyridine H), 3.72 (s, 8H; NH-CH_2-pyridine), 3.4–3.6 (m, 10H; CO-CH(R)-CO + CO-NH-CH_2); 2.9–3.0 (m, 12H; C≡C-CH_2- + -CH_2-NH-CH_2), 1.9 ppm (br; HC≡C- + amine protons); MS (ESI): *m*/*z*: 659 [**L6**H_4+H^+]; elemental analysis calcd (%) for $C_{34}H_{50}N_{10}O_6$ (**L6**H_4+2H_2O): C 58.77, H 7.25, N 20.15; found: C 58.75, H 7.26, N 20.14.

Potentiometric titrations: Protonation equilibria of ligands **L1**H_2–**L3**H_2, **L5**H_4, and **L6**H_4 were studied in water containing $NaNO_3$ (0.05 M), thermostatted at 25 °C, with a Radiometer automatic titrating system (Titralab TIM900) kept under a nitrogen atmosphere. In a typical experiment, 30–50 mL of a 10^{-3} M ligand solution was treated with 1.0 M standard HNO_3 in a molar quantity corresponding to the moles of ligand multiplied by the number of basic groups (amines+quinolines or pyridines) augmented by 2. Titrations were run by additions of 10–20 μL portions of standard 0.1 M NaOH, collecting 80—100 points for each titration. Complexation equilibria were studied by means of titrations run under the same conditions, except that the starting solution also contained [Cu-(CF_3SO_3)$_2$] in a 1:1 (**L1**H_2–**L3**H_2) or 2:1 (**L5**H_4, **L6**H_4) molar ratio with respect to the ligand. Prior to each potentiometric titration, a titration according to the Gran method[18] was run to determine the $E°$ of the glass electrode under the chosen conditions. Protonation data (emf versus volume of added base) were processed with the Hyperquad package[9] to determine protonation constants. After determination of the protonation

constants, emf versus volume of added base data obtained in the presence of Cu^{2+} were used to determine the formation constants of the metal–ligand species. Potentiometric titrations for **L4**H_2 (both in the absence and in the presence of $[Cu(CF_3SO_3)_2]$ in a 1:1 molar ratio) were run in dioxane/water (8:2 v/v) under the same conditions.

Spectrophotometric titrations: Coupled spectrophotometric/pH-metric titrations were run with a procedure and under conditions similar to that described for the potentiometric titrations. However, in this case, standard base was added manually, by means of a 10 or 20 μL Rainin pipet-lite pipette. After each addition, a portion of the solution was transferred into a quartz cuvette and its absorption spectrum recorded. After the spectrum was recorded, the solution was transferred back to the bulk titrated solution. The spectra recorded after each addition were associated with a pH value measured in the bulk solution by means of a glass electrode.

Electrochemistry: Cyclic voltammetric measurements were run in a three-electrode cell, using a saturated calomel electrode (SCE) as the reference, a glassy carbon electrode as the working electrode, and a platinum wire as the counter electrode. Water containing $NaNO_3$ (0.1 M) was used as solvent (in the case of CV run on Cu^{2+} **L4**H_2 complexes, dioxane/water 8:2 v/v was used as the solvent, $NaNO_3$ as the background electrolyte, and a Ag/AgCl electrode as the reference). Ligand + metal solutions were at concentrations ≥ 0.001 M. The pH was regulated by means of microadditions of standard base or acid, and checked with a glass electrode dipped in the electrochemical solution before any measurements. Scan rates were in the 50–400 $mV\,s^{-1}$ range.

Instrumentation: UV/Vis spectra were run with a diode array HP8452 spectrophotometer and with a Varian Cary 1000 SCAN spectrophotometer. Electrochemistry was obtained with a BAS 100B/W instrument. Mass spectra were recorded on a Finnigan MAT TSQ 700 instrument, NMR spectra on a Bruker AMX 400. IR spectra were taken on a Mattson 5000 instrument. Automatic potentiometric titrations were run with a Radiometer Titralab TIM900 apparatus with dedicated software.

X-ray crystallographic studies: Diffraction data were collected at ambient temperature by using an Enraf–Nonius CAD4 four-circle diffractometer with graphite-monochromatized $Mo_{K\alpha}$ radiation ($\lambda = 0.7107$ Å). Crystal data for {[**L1**Cu]·2H_2O} and {[**L6**Cu_2]·9H_2O} complexes are reported in Table 2. Data reductions (including intensity integration, background, Lorentz, and polarization corrections) were performed with the WinGX package.[19] Absorption effects were evaluated with the psi-scan method[20] and absorption correction was applied to the data (min./max. transmission factors were 0.376/0.560 for [**L1**Cu] and 0.789/0.853 for [**L6**Cu_2]).

Crystal structures were solved by direct methods (SIR 97)[21] and refined by full-matrix least-square procedures on F^2 using all reflections (SHELXL 97).[22] Anisotropic displacement parameters were refined for all non-hydrogen atoms. For both complexes, hydrogen atoms bonded to the ligand moiety were placed at calculated positions with the appropriate AFIX instructions and refined by using a riding model. Hydrogen atoms of water molecules were located in the ΔF map and refined with soft restraint on the O–H distance. The quality of the crystal of complex [**L6**Cu_2] did not allow us to define the position of hydrogen atoms bonded to the O(8), O(9), and O(10) water oxygen atoms. Furthermore, the C(32)-C(33)-C(34) propargyl group and the O(9) atom in the [**L6**Cu_2] crystal result were disordered over two alternative positions with the same statistical probability.

CCDC-278522 and CCDC-278523 contains the supplementary crystallographic data for this paper. These data can be obtained free of charge from The Cambridge Crystallographic Data Centre via www.ccdc.cam.ac.uk/data_request/cif.

Acknowledgements

This work was financially supported by the Università di Pavia (FAR 2004) and by MIUR program (project FIRB RBNE019H9K-002 and COFIN2003 National Program)

[1] a) H. A. O. Hill, K. A. Raspin, *J. Chem. Soc. A* **1968**, 3036; b) M. Kodama, E. Kimura, *J. Chem. Soc. Dalton Trans.* **1979**, 325.
[2] a) M. Kodama, E. Kimura, *J. Chem. Soc. Dalton Trans.* **1979**, 1783; b) M. Kodama, E. Kimura, *J. Chem. Soc. Dalton Trans.* **1981**, 684; c) E. Kimura, A. Sakonaka, R. Machida, M. Kodama, *J. Am. Chem. Soc.* **1982**, *104*, 4255; d) R. Machida, E. Kimura, M. Kodama, *Inorg. Chem.* **1983**, *22*, 2055.
[3] a) L. Fabbrizzi, A. Poggi, *J. Chem. Soc. Chem. Commun.* **1980**, 646; b) L. Fabbrizzi, A. Perotti, A. Poggi, *Inorg. Chem.* **1983**, *22*, 1411; c) E. Kimura, T. Koike, R. Machida, R. Nagai, M. Kodama, *Inorg. Chem.* **1984**, *23*, 4181.
[4] a) L. Fabbrizzi, M. Licchelli, P. Pallavicini, A. Perotti, D. Sacchi, *Angew. Chem.* **1994**, *106*, 2051; *Angew. Chem. Int. Ed. Engl.* **1994**, *33*, 1975; b) L. Fabbrizzi, M. Licchelli, P. Pallavicini, A. Perotti, A. Taglietti, D. Sacchi, *Chem. Eur. J.* **1996**, *2*, 75; c) F. Bolletta, I. Costa, L. Fabbrizzi, M. Licchelli, M. Montalti, P. Pallavicini, L. Prodi, N. Zaccheroni, *J. Chem. Soc. Dalton Trans.* **1999**, 1381; d) Y. Diaz Fernandez, A. Perez Gramatges, V. Amendola, F. Foti, C. Mangano, P. Pallavicini, S. Patroni, *Chem. Commun.* **2004**, 1650.
[5] a) G. De Santis, L. Fabbrizzi, M. Licchelli, P. Pallavicini, A. Perotti, *J. Chem. Soc. Dalton Trans.* **1992**, 3283; b) G. De Santis, L. Fabbrizzi, M. Licchelli, P. Pallavicini, A. Perotti, A. Poggi, *Supramol. Chem.* **1994**, *3*, 115.
[6] a) V. Amendola, L. Fabbrizzi, C. Mangano, P. Pallavicini, A. Perotti, A. Taglietti, *J. Chem. Soc. Dalton Trans.* **2000**, 185; b) V. Amendola, L. Fabbrizzi, C. Mangano, P. Pallavicini, *Acc. Chem. Res.* **2001**, *34*, 488; c) V. Amendola, C. Brusoni, L. Fabbrizzi, C. Mangano, H. Miller, P. Pallavicini, A. Perotti, A. Taglietti, *J. Chem. Soc. Dalton Trans.* **2001**, 3528; d) V. Amendola, L. Fabbrizzi, C. Mangano, H. Miller, P. Pallavicini, A. Perotti, A. Taglietti, *Angew. Chem.* **2002**, *114*, 2665; *Angew. Chem. Int. Ed.* **2002**, *41*, 2553.
[7] L. Fabbrizzi, F. Foti, S. Patroni, P. Pallavicini, A. Taglietti, *Angew. Chem.* **2004**, *116*, 5183; *Angew. Chem. Int. Ed.* **2004**, *43*, 5073.
[8] a) This research group is involved in a long-term project dedicated to the preparation and electrochemical study of SAM of metal complexes on Si surfaces, see: E. A. Dalchiele, A. Aurora, G. Bernardini, F. Cattaruzza, A. Flamini, P. Pallavicini, R. Zanoni, F. Decker, *J. Electroanal. Chem.* **2005**, *579*, 133; b) E. G. Robins, M. P. Stewart, J. M. Buriak, *Chem. Commun.* **1999**, 2479; P. T. Hurley, A. E. Ribbe, J. M. Buriak, *J. Am. Chem. Soc.* **2003**, *125*, 11334
[9] P. Gans, A. Sabatini, A. Vacca, *Talanta* **1996**, *43*, 1739.
[10] G. De Santis, L. Fabbrizzi, A. M. Manotti Lanfredi, P. Pallavicini, A. Perotti, F. Ugozzoli, M. Zema, *Inorg. Chem.* **1995**, *34*, 4529.
[11] L. Ilcheva, J. Bjerrum, *Acta Chem. Scand.* **1976**, *30*, 343.
[12] R. Menif, J. Reibenspies, A. E. Martell, *Inorg. Chem.* **1991**, *30*, 3446.
[13] F. P. Bossu, K. L. Chellappa, D. W. Margerum, *J. Am. Chem. Soc.* **1977**, *99*, 2195.
[14] Y. D. Lampeka, S. P. Gavrish, *J. Coord. Chem.* **1990**, *21*, 351.
[15] J. P. Hinton, D. W. Margerum, *Inorg. Chem.* **1986**, *25*, 3248.
[16] G. Eglinton, M. C. Whiting, *J. Chem. Soc.* **1952**, 3052.
[17] H. G. Hamilton, Jr., M. D. Alexander, *Inorganic Chemistry, Vol. 5, no. 11*, **1966**, p. 2060.
[18] G. Gran, *Analyst (London)* **1952**, 77, 661.
[19] L. J. Farrugia, *J. Appl. Crystallogr.* **1999**, *32*, 837.
[20] A. C. T. North, D. C. Phillips, F. S. Mathews, *Acta. Crystallogr. Sect. A* **1968**, 24, 351.
[21] A. Altomare, M. C. Burla, M. Camalli, G. L. Cascarano, C. Giacovazzo, A. Guagliardi, A. G. G. Moliterni, G. Polidori, R. Spagna, *J. Appl. Crystallogr.* **1999**, *32*, 115.
[22] G. M. Sheldrick. SHELX97 Programs for Crystal Structure Analysis. University of Göttingen, Germany, **1997**.

Received: October 7, 2005
Revised: December 15, 2005
Published online: April 25, 2006

